Thermoremanent magnetization in Mn-rich $Cu_{100-x}Mn_x$ ($x=73$, 76, and 83) binary alloys

R. S. Patel
Physics Department, Indian Institute of Technology, Kanpur 208016, Uttar Pradesh, India

D. Kumar
Center for Advanced Materials and Smart Structures, Department of Mechanical Engineering, North Carolina State University, Raleigh, North Carolina 27695

A. K. Majumdar*
Department of Physics, University of Florida, Gainesville, Florida 32611
and Physics Department, Indian Institute of Technology, Kanpur 208016, Uttar Pradesh, India

(Received 9 November 2001; revised manuscript received 18 March 2002; published 5 August 2002)

$Cu_{100-x}Mn_x$ alloys in the dilute-spin-glass regime ($x \leqslant 10\%$) show stretched exponential relaxation of thermoremanent magnetization (TRM). Instead in the concentrated long-range-antiferromagnetic regime, we find that the TRM is described well by a power-law decay with faster relaxation at higher temperatures. Logarithmic decay plots show systematic curvature, the nature of which depends on the distribution of energy barriers over which magnetic relaxation takes place.

DOI: 10.1103/PhysRevB.66.054408 PACS number(s): 75.30.Kz, 75.50.Ee, 75.50.Lk

I. INTRODUCTION

$Cu_{100-x}Mn_x$ forms a solid solution over the whole concentration range. In an earlier work[1] we had established its magnetic phase diagram primarily through magnetic measurements. The alloys with $x \leqslant 73$ at. % had shown time- and history-dependent dc magnetization and peaks in ac susceptibility (χ_{ac}). The lower concentration ($x \leqslant 10$) alloys (cusp in χ_{ac}) are designated as spin glasses (SG's) and the higher ones (broad peaks in χ_{ac}) as cluster glasses (CG's) with T_f as their freezing temperatures (paramagnetic to SG or CG). For $x=76$ and 83 at. %, double transition from paramagnetic to antiferromagnetic ($T_N=275$ and 484 K) to a mixed cluster-glass-antiferromagnetic phase ($T_f=130$ and 45 K) were observed. Bifurcation of field-cooled (FC) and zero-field-cooled (ZFC) magnetization versus temperature curves showed very clearly the second transition at T_f for both $x=76$ and 83 at. % (Fig. 6 of Ref. 1). The existence of the mixed phase was concluded from the above magnetic studies and the neutron-diffraction measurements of Cowlam and Shamah.[2] The alloy with $x=73$ at. % seems to be very near to the multicritical concentration with $T_N=T_f \cong 160$ K. The alloys with $x \geqslant 73$ at. % have long-range type-1 antiferromagnetc structure (AF1) with tetragonal distortion whereas the alloys with $x<73$ at. % have short-range order based on type-3 antiferromagnetic structure (AF3).[2]

$Cu_{100-x}Mn_x$ binary alloys in the very dilute magnetic impurity limit ($x \leqslant 1\%$) show resistivity minima ($\rho \sim -\ln T$ below T_{min}) at very low temperatures which are interpreted in terms of Kondo effect.[3] The composition region until $x \simeq 30$ at. % shows a monotonic decrease of the electrical resistivity with the decrease of temperature all the way down to very low temperatures. However, resistivity minima were observed by us[4] again at higher concentrations between $x=36$ and 83 at. % with T_{min} lying between 2 and 25 K. Here $\rho \sim -\sqrt{T}$ (below T_{min}) and these minima were interpreted in terms of the electron-electron interaction in the presence of weak localization. In this report we investigate the time dependence of the dc magnetization of the more concentrated $Cu_{100-x}Mn_x$ alloys with $x=73$, 76, and 83.

Thermoremanent magnetization (TRM) in different magnetic phases has been recently summarized and studied in $\gamma-Fe_{80-x}Ni_xCr_{20}$ ($14 \leqslant x \leqslant 30$) alloys showing antiferromagnetic, spin-glass, re-entrant spin-glass, and ferromagnetic phases as x is varied.[5] Several theoretical models have been discussed for the time dependence of magnetization (see Ref. 5 and references therein). Early decay measurements in spin glasses had shown logarithmic relaxation given by[6]

$$M(t)=M_0-S\ln(t), \tag{1}$$

where M_0 is a parameter and S is the logarithmic decay rate which is a measure of the magnetic viscosity that slows down the decay rate. A single energy barrier leads to an exponential relaxation whereas a summation over the distribution of energy barriers (giving rise to a distribution of relaxation times) produces a logarithmic decay [Eq. (1)]. Later measurements in spin glasses and presumably cluster glasses had shown a more complicated stretched exponential (anomalously slow) multiplied by a power-law (aging effect) behavior, given by[7]

$$M(t)=M_0\left(\frac{t}{t_w}\right)^{-\gamma}\exp\left[-\left(\frac{t}{\tau}\right)^{1-n}\right], \tag{2}$$

where t_w is the wait time (time of exposure in a magnetic field) below T_f (spin-glass freezing temperature), τ is the characteristic relaxation time, and M_0, γ, and n are parameters. For antiferromagnets,[5] stretched exponential decay (no aging effect) like

$$M(t)=M_0\exp\left[-\left(\frac{t}{\tau}\right)^{\beta}\right], \tag{3}$$

where τ is the relaxation time and M_0 and β are parameters or power-law decay of the form

$$M(t) = M_0 t^{-\gamma}, \tag{4}$$

where M_0 and γ are parameters, fits equally well.

II. EXPERIMENTAL DETAILS

In view of the above facts, we have made a detailed study of the time-dependent magnetization in Mn-rich $Cu_{100-x}Mn_x$ alloys ($x=73$, 76, and 83). The alloys were prepared by induction melting in a pure argon atmosphere of spectroscopically pure Cu and Mn as described in details elsewhere.[1] We have studied the time dependence of TRM using a superconducting quantum interference device (SQUID) magnetometer (Quantum Design MPMS) in the following way. We cooled the sample in a field of 1000 Oe from room temperature to a fixed temperature (T), kept the magnetic field for a fixed time, defined as wait time t_w, which includes the cooling time from their respective T_N's to T and attain equilibrium. Then we switched off the field and started the measurement of the decaying magnetic moment as a function of time after the field became zero (~ 1 min). For each sample we did the experiment in two ways. First, we had kept the temperature constant at 10 K and took measurements for different t_w. Next, we had kept the waiting time constant at $t_w = 30$ min and repeated the experiment for different temperatures. This cooling time decreases as the measuring temperature increases and this has been properly incorporated in t_w. As an example, it took 20 min to reach 30 K for sample 2 and so we kept the magnetic field on for another 10, 40, 70, and 130 min so that $t_w = 30$, 60, 90, and 150 min.

III. RESULTS AND DISCUSSION

Time dependence of magnetization in dilute CuMn alloys in the spin-glass regime have been extensively studied. One such study had shown stretched exponential behavior [Eq. (3)] with $1/\tau$ varying exponentially with the inverse reduced temperature for all $T < T_f$ for $Cu_{96}Mn_4$ alloy.[8] Stretched exponential behavior had also been observed in other compositions like $Cu_{99}Mn_1$ and $Cu_{94}Mn_6$.[9] For the present concentrated Mn alloys we first tried the stretched exponential fit in the form of Eq. (3) for the magnetization M at several temperatures (for a constant wait time of 30 min) against time. We have used a standard nonlinear least-squares-fit program for all the three samples. The stretched exponential fits give very low χ^2 values consistent with the experimental resolution (typically 1 part in 10^4 of M at 10 K) and correlation coefficients of ~ 0.999 but the values of the parameters come out to be unrealistic and also they vary widely with error bars far exceeding the values themselves. χ^2 is defined as

$$\chi^2 = \frac{1}{N} \sum_{i=1}^{N} \frac{(M_{i_{measured}} - M_{i_{fitted}})^2}{M_{i_{mean}}^2}. \tag{5}$$

The parameter τ, according to our expectation, should be of the order of $\sim 10^4$–10^8 sec. It comes out to be $\sim 10^{20}$ sec which is unphysically long and with error bars of the same order. This is the case for all the three compositions.

TABLE I. $x=73$. Values of χ^2 and correlation coefficient r^2 and the parameters M_0 and γ of Eq. (4) for sample 1 ($Cu_{27}Mn_{73}$). T was varied for a constant wait time of 30 min, then t_w was varied at a constant temperature of 10 K.

T (K)	χ^2	r^2	M_0 (10^{-3} emu/g)	γ (10^{-5})
10	1.622×10^{-8}	0.997	6.112 ± 0.001	189 ± 2
50	4.481×10^{-5}	0.987	1.774 ± 0.010	4680 ± 90
100	1.379×10^{-4}	0.997	0.481 ± 0.005	15530 ± 140
150	1.863×10^{-3}	0.975	0.01 ± 0.004	20460 ± 520
t_w (min)	χ^2	r^2	M_0 (10^{-3} emu/g)	γ (10^{-5})
30	1.231×10^{-8}	0.998	6.2230 ± 0.0007	222 ± 1
45	2.072×10^{-8}	0.998	6.2305 ± 0.0009	238 ± 2
60	1.770×10^{-8}	0.998	6.2373 ± 0.0008	244 ± 2
90	2.24×10^{-8}	0.988	6.2411 ± 0.0009	255 ± 2

However, we found, for all the three samples at several temperatures but constant wait time of 30 min, that the power law in the form of Eq. (4) gives excellent results. These fits yield correlation coefficients >0.99, χ^2 values comparable with the experimental resolution and more importantly very small ($\sim 1\%$) error bars in the values of the parameters M_0 and γ. These values are compiled in Tables I, II, and III for samples with $x=73$, 76, and 83, which are designated as samples 1, 2, and 3, respectively. Variations are shown as functions of T ($t_w = 30$ min) and t_w ($T = 10$ K). It is very clear from the values of χ^2 and correlation coefficients given in Tables I–III that the fits to the power-law decay are better at lower temperature for all the samples. The fits at a given temperature improve as x increases, i.e., for samples with stronger long-range-antiferromagnetic order (AF1 structure). These fits are shown in Fig. 1 where M is plotted against time t for $t_w = 30$ min for all the three

TABLE II. $x=76$. Values of χ^2, correlation coefficient r^2, and the parameters M_0 and γ of Eq. (4) for sample 2 ($Cu_{24}Mn_{76}$). T was varied for a constant wait time of 30 min, then t_w was varied at a constant temperature of 10 K.

T (K)	χ^2	r^2	M_0 (10^{-3} emu/g)	γ (10^{-5})
10	9.99×10^{-9}	0.999	7.551 ± 0.001	310 ± 1
20	1.007×10^{-7}	0.998	6.569 ± 0.002	608 ± 4
30	2.517×10^{-7}	0.998	5.037 ± 0.003	970 ± 6
40	3.946×10^{-6}	0.997	1.855 ± 0.004	2720 ± 30
60	1.509×10^{-4}	0.975	1.034 ± 0.03	14800 ± 400
t_w (min)	χ^2	r^2	M_0 ($\times10^{-3}$ emu/g)	γ (10^{-5})
30	1.093×10^{-8}	0.998	8.248 ± 0.001	256 ± 1
60	3.375×10^{-8}	0.998	8.305 ± 0.002	310 ± 2
90	3.299×10^{-8}	0.998	8.315 ± 0.001	321 ± 2
150	3.983×10^{-8}	0.997	8.318 ± 0.002	324 ± 3

TABLE III. $x=83$. Values of χ^2, correlation coefficient r^2, and the parameters M_0 and γ of Eq. (4) for sample 3 ($Cu_{17}Mn_{83}$). T was varied for a constant wait time of 30 min, then t_w was varied at a constant temperature of 10 K.

T	χ^2	r^2	M_0 (10^{-3} emu/g)	γ (10^{-5})
10	2.164×10^{-8}	0.999	10.187 ± 0.002	342 ± 2
15	6.453×10^{-8}	0.998	9.541 ± 0.002	485 ± 3
20	6.719×10^{-8}	0.999	8.798 ± 0.002	606 ± 3
25	9.935×10^{-8}	0.999	7.870 ± 0.003	752 ± 4
30	4.986×10^{-8}	0.999	6.556 ± 0.002	850 ± 3
35	1.809×10^{-8}	0.999	4.594 ± 0.001	1080 ± 3
40	6.856×10^{-7}	0.999	1.263 ± 0.001	2090 ± 10
t_w (min)	χ^2	r^2	M_0 (10^{-3} emu/g)	γ (10^{-5})
30	7.769×10^{-9}	0.999	10.172 ± 0.001	335 ± 1
45	1.323×10^{-8}	0.999	10.214 ± 0.001	389 ± 1
60	3.248×10^{-8}	0.998	10.221 ± 0.002	390 ± 2
90	6.409×10^{-8}	0.997	10.247 ± 0.003	405 ± 3

samples at 10 K. The solid lines are the best-fitted curves. It is to be noted here that the magnetization decays by atmost $1\frac{1}{2}\%$ in three decades of time in any of the three samples shown in Fig. 1. The sensitivity of the SQUID magnetometer makes this kind of high-resolution measurement possible. For the power-law fit, the parameter M_0, which is the magnetization at very small times, decreases with temperature for $t_w=30$ min as shown in Fig. 2 for all the three samples. This is expected because higher temperatures reduce the thermoremanent magnetization. From Tables I–III we find that at $T=10$ K and $t_w=30$ min, $M_0=6.1$, 7.6 and 10.2 (10^{-3} emu/g) for $x=73$, 76, and 83, respectively. In other words, the field-cooled moment M_0 increases with x. This can be understood in terms of the details of the AF1 and AF3 structures.[2] In the AF3 structure ($x\leqslant73$), both the nearest-neighbor (J_1) and the next-nearest-neighbor (J_2) interactions of Mn are antiferromagnetic while for the AF1 structure ($x\geqslant73$, the present set of alloys) J_1 is antiferromagnetic whereas J_2 is ferromagnetic. In addition J_2 is found to be almost twice J_1. It is also found that the average number of Mn next-nearest neighbors is large compared to those of the nearest neighbors. As a result J_2 aligns some of the random moments enhancing M_0 with x.

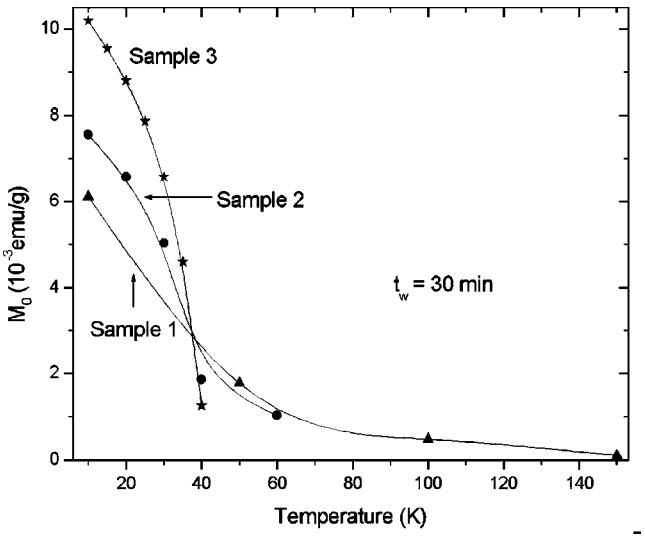

FIG. 2. Variation of the parameter M_0 of Eq. (4) with temperature for the three samples. The solid lines are just guides to the eye. M_0, the value of the magnetization at very small times, decreases with temperature for each sample. M_0 at the lowest temperature (10 K) increases with the Mn concentration x ($x=73$, 76, and 83 for samples 1, 2, and 3, respectively).

The exponent γ increases with temperature as shown in Fig. 3 for all the three samples. This is well understood since the relaxation of magnetization is expected to be faster at higher temperatures. A closer look at Fig. 3, specially the curve for sample 3, shows that γ increases roughly linearly with T until 30 K and then it diverges at 40 K which is just

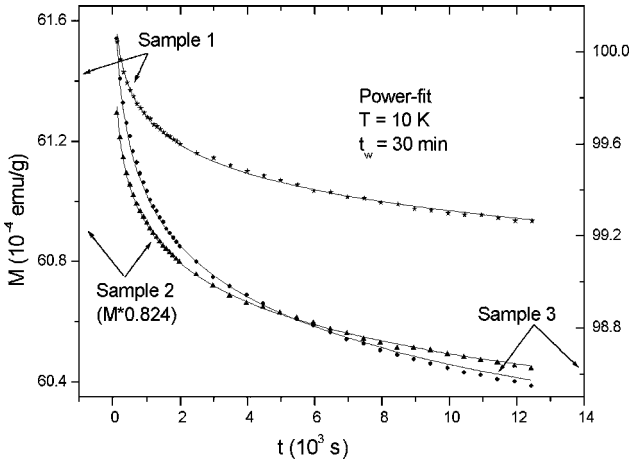

FIG. 1. M is plotted against time, t for the three samples at 10 K and wait time of 30 min. The solid lines are the power-law fits [Eq. (4)].

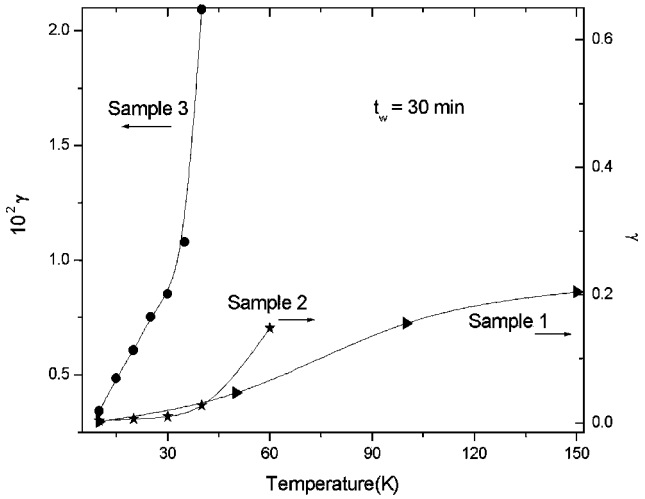

FIG. 3. Variation of the exponent γ of Eq. (4) with temperature for the three samples. The solid lines are just guides to the eye. The relaxation rate increases with the increase of temperature.

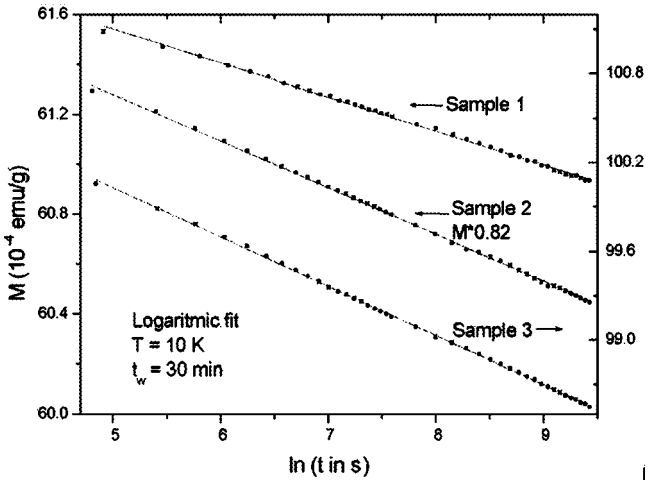

FIG. 4. M is plotted against ln (t in sec) for the three samples at 10 K and wait time of 30 min. The solid lines are the logarithmic fits [Eq. (1)].

below its T_f of 45 K. This kind of divergence of the exponent γ was found in insulating spin glasses around T_f.[10] This linear variation of γ is consistent with the Monte Carlo simulations[11] for a two-dimensional (2D) Ising spin glass for $T \ll T_f$. However, the power law does not hold around T_f where γ is found to show divergence as in our investigation as well (see Fig. 3 and Tables I–III). As depicted in Fig. 3, this divergence of $\gamma(T)$ is also clear for sample 2 at 60 K ($T_f = 130$ K) but not in sample 1 since we have not gone above its T_f of 160 K. Similar linear behavior of $\gamma(T)$ was predicted[12] in spin glasses using a simple picture of the decay of total magnetization through flipping of independent spins and clusters by climbing over energy barriers.

Equally good fits are obtained when $M(t)$ is fitted to Eq. (4) at a constant temperature of 10 K at several values of t_w.

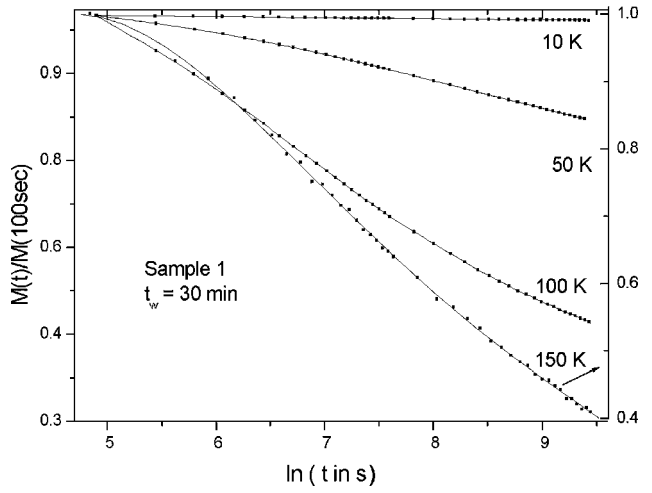

FIG. 5. Raw data points of normalized magnetic moment $M(t)/M(100 \text{ sec})$ at different temperatures vs ln (t in sec) for $t_w = 30$ min for sample 1. The data are linear at 10 K (see Fig. 4 for an expanded M axis) and show deviations from linearity [deviation from Eq. (1)] at 50, 100, and 150 K. The solid lines are just guides to the eye.

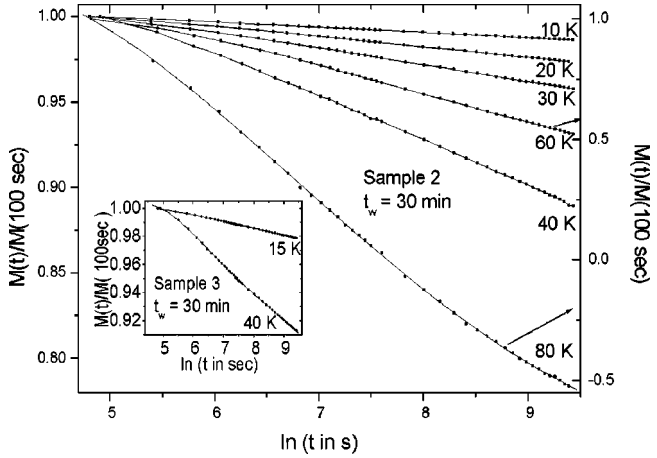

FIG. 6. Same as in Fig. 5 except here for sample 2. Deviations from linearity are observed between 20 and 80 K. The solid lines are just guides to the eye. The negative value of $M(t)/M(100 \text{ sec})$ at larger times for the highest temperature of 80 K is due to the relatively large diamagnetic correction from the sample holder. The inset shows similar convex upwards behavior at $T = 15$ K and mixed curvature at $T = 40$ K for sample 3.

The details of the fits are given in Tables I–III. Very similar conclusions were reached in an antiferromagnetic FeNiCr alloy.[5] It should be noted here that all the three alloys in the present investigation have long-range-antiferromagnetic order. However, in an earlier work Ikeda and Kikuta[13] could not find any relaxation of TRM over a period of 10 h in the antiferromagnet $Mn_{0.45}Zn_{0.55}F_2$ for $T < T_N$.

Néel's theory of superparamagnetism[14] gives a reasonably good qualitative agreement with the observed magnetic properties in these Mn-rich CuMn alloys.[1] It is similar to the phenomenon of blocking of superparamagnetic particles in rock magnetism.[15] Here, the magnetic material is thought to be made up of magnetic clusters of various sizes (v), coercive field (H_c)/anisotropy energy, and spontaneous magneti-

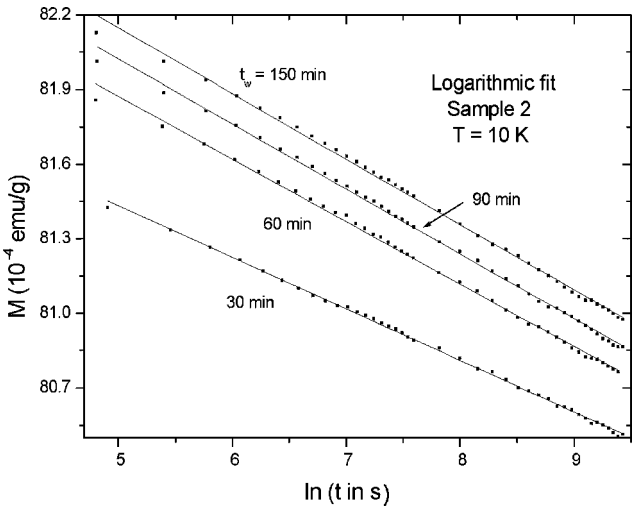

FIG. 7. M is plotted against ln (t in sec) for sample 2 at 10 K for wait times $t_w = 30$, 60, 90, and 150 min. The solid lines are the logarithmic fits [Eq. (1)].

zation (M_s). The anisotropy acts like a potential barrier for the cluster magnetization to relax. The thermal activation of the cluster magnetization over these barriers leads to an exponential relaxation of TRM, viz., $M(t) \sim \exp(-t/\tau)$ where the relaxation time $\tau \sim \exp(\triangle E/k_B T)$, where the height of the barrier $\triangle E = v H_c M_s/2$. A distribution of barrier heights (due to distributions of v, H_c, and M_s) implies a distribution of blocking temperatures, only above which individual magnetic clusters have sufficient thermal energy to relax. This distribution of barrier heights finally yields a logarithmic decay of M as given in Eq. (1). So, we next tried to fit our data for all the samples at several temperatures to Eq. (1). Except at the lowest temperature of 10 K, the logarithmic plots show a systematic curvature indicating deviations from Eq. (1). Figure 4 shows fits of M vs $\ln(t)$ data at 10 K and $t_w = 30$ min for all the samples. The best-fitted curves (solid lines) are straight lines in agreement with Eq. (1) and χ^2 values of $\sim 10^{-8}$ consistent with the experimental resolution of M (1 part in 10^4), correlation coefficient >0.998, and errors in the values of the coefficients of less than 1%. This linear dependence of M versus $\ln(t)$ implies that the barrier height distribution in approximately independent of time.

$M(t)/M(100\ \text{sec})$ vs $\ln(t)$ data for $t_w = 30$ min at $T = 10$, 50, 100, and 150 K for sample 1 are plotted in Fig. 5. $M(t)$ data are normalized by dividing by $M(100$ sec) at each temperature to bring them on a common scale. The data are linear at 10 K (see Fig. 4 for an expanded M axis) in agreement with Eq. (1). At higher temperatures, however, there are deviations from $M(t) \sim \ln(t)$ behavior, i.e., Eq. (1). At 50 K, $M(t)$ is convex upwards whereas at 100 and 150 K, $M(t)$ is convex upwards for shorter time and concave upwards for longer time. In a recent theoretical paper O'Grady, El-Hilo, and Chantrell[16] had predicted a very similar behavior of thermoremanent magnetization based on the relaxation of magnetic moments over a narrow distribution of energy barriers (see Fig. 1 of Ref. 16). They found that the $M(t)$ vs $\ln(t)$ curve is convex upwards (similar to our 50-K data shown in Fig. 5) if the ''relaxation takes place over barriers less than the average barrier.'' For barriers close to the average barrier, the $M(t)$ vs $\ln(t)$ curve shows both convex and concave upwards behavior for small and large times, respectively, very similar to our 100- and 150-K data shown in Fig. 5 for sample 1. However, we did not observe the third possibility for barriers greater than the average barrier where $M(t)$ vs $\ln(t)$ is predicted to be concave upwards for all times.

Similar behavior is seen in Fig. 6 for sample 2 where $M(t)/M(100\ \text{sec})$ vs $\ln(t)$ data are shown at several temperatures. The plot is more or less linear at 10 K, shows convex upwards behavior at 20, 30, and 40 K and mixed curvature at 60 and 80 K. The negative values of $M(t)/M(100$ sec) at larger times for the highest temperature of 80 K is due to the relatively large diamagnetic correction from the sample holder. The inset of Fig. 6 shows similar convex upwards behavior at $T = 15$ K and mixed curvature at $T = 40$ K for sample 3. So we find that the deviation from linearity in $M(t)$ vs $\ln(t)$ plot is quite a general one and $T \sim 50$ K is the temperature which separates the two temperature regimes giving different curvatures, as observed in Figs. 5 and 6. $S(t) = dM(t)/d(\ln(t))$ [Eq. (1)] plots (not shown) show peaks around $t \cong t_w$ for those temperatures where $M(t)$ curves have mixed curvatures.

In Fig. 7 we have plotted M vs $\ln(t)$ for sample 2 at 10 K for different wait times of 30, 60, 90, and 150 min. The solid lines are the best-fitted curves for fit to Eq. (1), viz., the logarithmic decay. As before logarithmic fits are quite satisfactory at low temperatures (say, 10 K here). However, they show deviations from linearity for higher t_w, just like those at higher temperatures for $t_w = 30$ min (as shown in Figs. 5 and 6).

IV. CONCLUSIONS

To conclude, instead of a stretched exponential decay of the TRM in the spin-glass regime, $Cu_{100-x}Mn_x$ ($x = 73$, 76, and 83) alloys in the long-range-antiferromagnetic state follow power-law decay. The TRM plotted against $\ln(t)$ shows systematic curvature as a function of temperature due to a distribution of energy barriers.

ACKNOWLEDGMENTS

R.S.P. acknowledges CSIR, Government of India, for financial support. A.K.M. acknowledges the Physics Department, University of Florida, Gainesville for local hospitality and experimental facilities. Financial support from DOD/AFOSR MURI Grant No. F49620-96-1-0026) is gratefully acknowledged. Special thanks go to A. F. Hebard for his constant encouragement and help.

*Author to whom correspondence should be addressed. Electronic address: akm@iitk.ac.in

[1] A. Banerjee and A. K. Majumdar, Phys. Rev. B **46**, 8958 (1992).
[2] N. Cowlam and A. M. Shamah, J. Phys. F: Met. Phys. **11**, 27 (1981).
[3] J. Kondo, Prog. Theor. Phys. **32**, 37 (1964).
[4] S. Chakraborty and A. K. Majumdar, Phys. Rev. B **53**, 6235 (1996).
[5] G. Sinha, R. Chatterjee, M. Uehara, and A. K. Majumdar, J. Magn. Magn. Mater. **164**, 345 (1996).
[6] R. Street and J. C. Woolley, Proc. Phys. Soc., London, Sect. A **62**, 562 (1949); Proc. Phys. Soc. London, Sect. B **69**, 1189 (1956).
[7] K. H. Fischer and J. A. Hertz, *Spin Glasses* (Cambridge University Press, Cambridge, England, 1991).
[8] R. Hoogerbeets, Wei-Li Luo, and R. Orbach, Phys. Rev. B **34**, 1719 (1986).
[9] R. V. Chamberlin, G. Mozurkewich, and R. Orbach, Phys. Rev. Lett. **52**, 867 (1984); D. Chu, G. G. Kenning, and R. Orbach, *ibid.* **72**, 3270 (1994).
[10] J. Ferré, J. Rajchenbach, and H. Maletta, J. Appl. Phys. **52**, 1697 (1981).
[11] W. Kinzel, Phys. Rev. B **19**, 4595 (1979).
[12] Chandan Dasgupta, Shang-keng Ma, and Chin-Kun Hu, Phys. Rev. B **20**, 3837 (1979).

[13] H. Ikeda and K. Kikuta, J. Phys. C **17**, 1221 (1984).
[14] L. Néel, Adv. Phys. **4**, 191 (1955).
[15] J. L. Tholence and R. Tournier, J. Phys. (Paris), Colloq. **35**, C4-229 (1974); Physica C **86-88B**, 873 (1977); E. P. Wohlfarth, Phys. Lett. A **70**, 489 (1979); J. Phys. F: Met. Phys. **10**, L241 (1980).
[16] K. O'Grady, M. El-Hilo, and R. W. Chantrell, J. Appl. Phys. **76**, 6368 (1994).